New Horizons in Earth Reinforcement – Otani, Miyata & Mukunoki (eds)
© 2008 Taylor & Francis Group, London, ISBN 978-0-415-45775-0

Resistance of steel chain in pullout tests with and without sliding box

M. Fukuda & T. Hongo
Geo-Research Institute, Japan

A. Kitamura & Y. Mochizuki
Showa Kikai Shoji, Japan

S. Inoue & E. Fujimura
Kinki Polytechnic College, Japan

M. Kimura
Kyoto University, Japan

ABSTRACT: Notable features of a steel chain are its flexibility in surrounding a deformed soil and a high pullout resistance larger than those expected from steel bars and plates. However, little is known about its mechanism of the pullout resistance. Therefore, a new experimental apparatus is developed to support the experienced hypothesis on the pullout resistance. This new apparatus also makes it possible to measure the pullout resistance under a high axial tensile force at a low confining pressure, which is commonly observed in the back fill of a retaining wall. In this study, two test procedures are conducted separately. One measures the resistance using a simple pullout test and the other one with a sliding box. This paper shows the parametric test results examined by combining chain shape, strip, plate and round bar with representative soils, relative density and confining pressure. Also, similar behaviour in resistance displacement curve is shown by comparing both test results.

1 INTRODUCTION

Design method for steel chain as a reinforcement material developed to stabilize fill slope has not been yet established even though the chain has an effective rigidity and shape with respect to pullout resistance. Therefore, to account for the pullout resistance characteristic of the steel chain, based on experimental fact data, a chain pullout testing device was developed. Various expected test conditions in practice were examined with this apparatus using chains of different shape and length, and comparative study done with steel plates with smooth surface with small projections, and round steel bars for different soils ranging from coarse to fine.

Moreover, this testing apparatus is added to have an advanced procedure to slide the surrounding soil in a container box along the steel chain under high axial tension and low confining pressure. This operation is aimed at studying the pullout resistance characteristic observed within the back fill of a reinforced retaining wall. Herein, two types of test are defined, a standard type test and a sliding box test. The complicated behaviour in the region close to the retaining wall is impossible to reproduce by the standard test in general. In this paper, basic equations that govern the pullout resistance of the steel chain are derived from the standard test by considering the effect of internal friction angle and dilatancy. Furthermore, confining pressure dependency and its correction method on the pullout resistance is introduced. Finally, the sliding box test results are indicated to follow the governing equations obtained from the standard test.

2 DEVELOPEMENT OF PULLOUT RESISTANCE UNDER HIGH AXIAL TENSION SITUATION

Axial tensile force reacting to geosynthetics materials in the back fill of a retaining wall is not of concerned in this research but only the pullout resistance generally localized in the vicinity of sliding surface in the reinforced fill far away from the retaining wall is focused on in this research.

Development of full resistance stretched over a total length of reinforcement is easily recognized to raise its function more efficiency in ideal. However, the lower

overburden pressure acting on reinforcement materials in the back fill of retaining wall and the shrinkage of the reinforcing materials lead to the neglecting of the resistance in the backfill. Therefore, to elaborate its reinforcement function, it is necessary to evaluate the sliding resistance in the back fill of the retaining wall.

3 CHAIN PULLOUT TEST APPARATUS AND ADDITIONAL DEVICES OF OUTER BOX SLIDING

A cubic container box for soils of dimension 50 cm × 50 cm × 50 cm with an inner volume of 0.125 m^3 that was about 10 times larger than the outer width of chain and the maximum diameter of the compacted soil particles used to conduct the test was designed as shown in Figure 2.

Five kinds of sensors are set up as load sensors for measuring vertical external pressure, there are also sensors for measuring the displacement of chains in the box, and earth pressure acting on chain in the soils and the side wall of the box.

The sliding box test is designed to measure pullout resistance of chain under high tensile force. Values of 12 kN and 15 kN of tensile force are chosen to act during the test since these values are considered to be a little bit lower than ultimate tensile strength of about 17 kN as recorded in Figure 3 for M624 (chain of 21 mm outer width). The testing materials were pulled out on three different confining pressures of 30, 90 and 150 kN/m^2 applied on the cover plate.

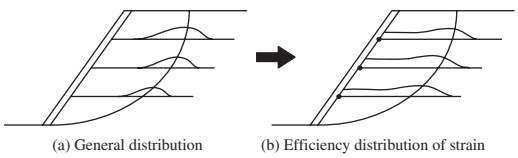

Figure 1. Wall confining effect and strain distribution pattern.

4 PULLOUT RESISTENCE AND CYLINDER MODEL

Equations (1) to (3) were proposed to predict the pull-out resistance of steel chain that assumes a cylindrical shape of soil block that envelop the inside space of the chain and outer surrounding soil. Figure 4 shows

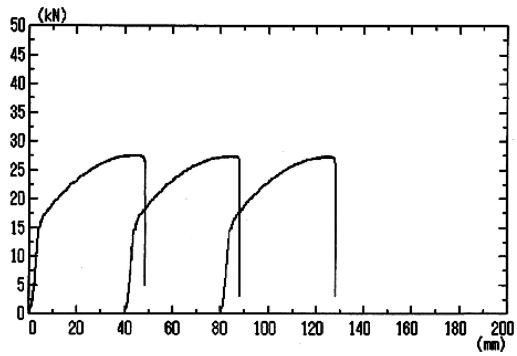

Figure 3. Tensile loading test result for chain.

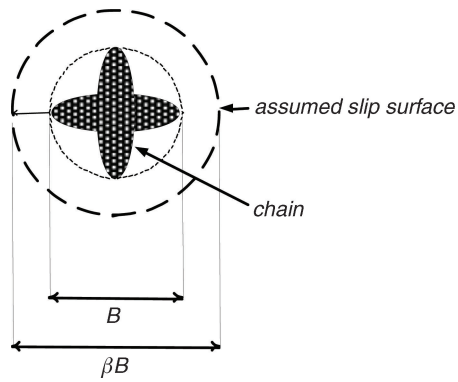

Figure 4. Cylinder model of sliding block attached to chain.

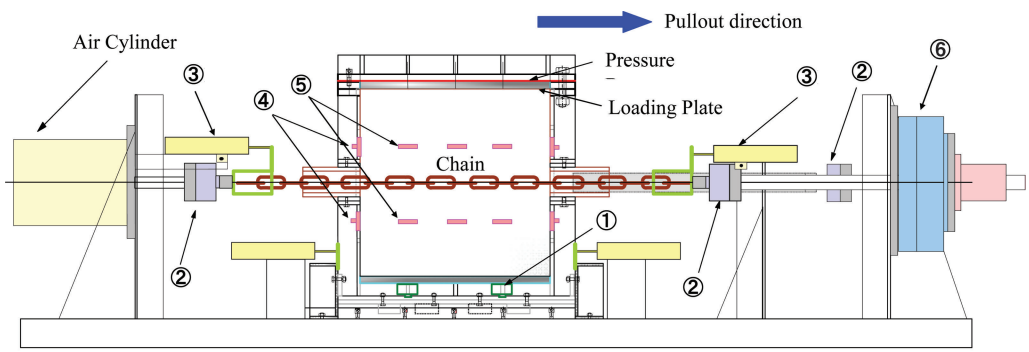

①,② Load Cell ③Displacement Indicator ④,⑤Earthpressure Cell

Figure 2. Schematic diagram of pullout testing apparatus.

the schematic diagram of sliding model used in this research.

$$F_f = \pi B \times \beta \times L \times \tan\phi' \times (1+K_0)/2 \times \sigma_v' \quad (1)$$

$$\alpha = \beta(1+K_0)/2 \quad (2)$$

$$F_f = \alpha \times \pi B \times L \times \sigma_v' \times \tan\phi' \quad (3)$$

Where F_f: pullout resistance, B: the outside width of the chain, ϕ: internal friction angle, K_0: lateral earth pressure coefficient, σ_v: effective vertical earth stress on the surface of chain, L: the chain length. Since F_f, B, L, and σ_v are directly obtained from the test results. Equation (3) is transformed to the equation (4) so as to obtain a factor α, the outer surface adjustment coefficient of the cylindrical model which is the targeted to of this research

$$\alpha = F_f/(\pi B \times L \times \sigma_v \times \tan\phi') \quad (4)$$

5 PULLOUT TEST CONDITION

5.1 *Filling material*

Figure 5 and Table 1 show physical properties of materials used for the tests. Toyoura sand compacted to 85% relative density, mixture filled with crushed stone and adjusted to diameters of 1 mm and 5 mm of 50% passing finer in weight compacted to 90% and 95% relative density and DL-clay and silica sand to 95% were used in this study.

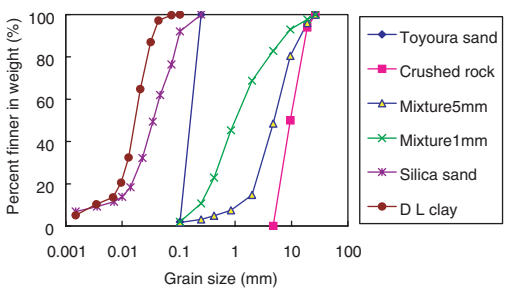

Figure 5. Grain size distribution curves of soils used for tests.

5.2 *Reinforcement materials used for test*

Since the purpose of the study was to investigate shape effect of chain on frictional resistance, chain of different shape and sizes were examined. Table 2 shows the dimensions of testing materials used in the study. Typical shape of the chain used in the study is as in shown in Figure 6. The outer width of the chains ranged from 1.5 cm to 3.1 cm.

A stripe steel plate of 3 mm high, steel plate of smooth surface 5 cm wide and a round steel bar of 2.2 cm in diameter used for comparative study are as shown in Photo 1.

6 BASIC PHENOMENA OF PULLOUT RESISTENCE

Figure 7 shows the pullout resistance obtained for different materials using the Toyoura sand filled in

Table 2. Chain specifications used for pull out tests.

No.	Name	Diameter D(mm)	Inner pitch p(mm)	Outer diameter b(mm)	links/ 50 cm
1	M6–Normal	6	24	21	21
2	M6–Long	6	37	21	14
3	M6–Short	6	18	21	28
4	M6–Wide	6	24	22.8	21
5	M6–Small	6	24	19.2	21
6	M6–Bar	6	24	21	21
7	M6–Knob	6	24	21	21
8	S6–24	6	24	21	21
9	L6–24	6	24	21	21
10	304–624S	6	24	21	21
11	M5–Square	4 × 5	19	15	18
12	B6–Cross	6	25.5	22	20
13	M8–38	8	38	31	14
14	L8–32	8	32	28	16

Table 1. Soil properties.

Material	Density of particle g/cm^3	Maximum dry density g/cm^3	Opitcal moisture %	Relative density %	Dry density g/cm^3	c′ kN/m^2	ϕ °
Crushed rock	2.661	1.696	5.6	95	1.61	26	39.2
Toyoura sand	2.65			85	1.58	4	37.9
Mixture 5 mm	2.656	1.927	8.3	95	1.83	13	41.4
				90	1.73	8	37.9
Mixture 1 mm	2.653	1.951	11.1	95	1.85	7	37.1
				90	1.76	5	35.9
Silica	2.634	1.365	10.3	90	1.23	4	33.8
DL clay	2.641	1.498	21.7	90	1.35	1	33.2

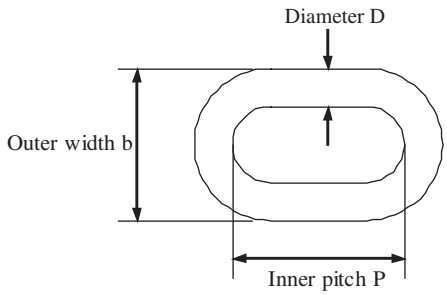

Figure 6. Shape definition of each chain.

Photo 1. Sub-materials used for comparative study.

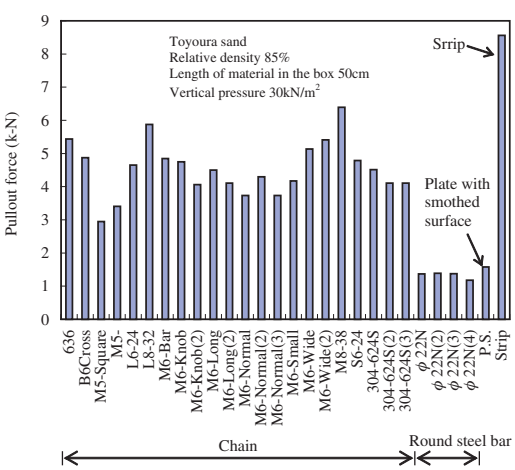

Figure 7. Pull out resistance obtained by pull out tests.

the testing box and compacted to 85% of the relative density under a vertical testing load of 30 kN/m^2.

Test results shows that the resistances of the chain ranged from 3 kN to 6 kN, on the other hand, the resistance of round steel bar was about 1 kN, while that

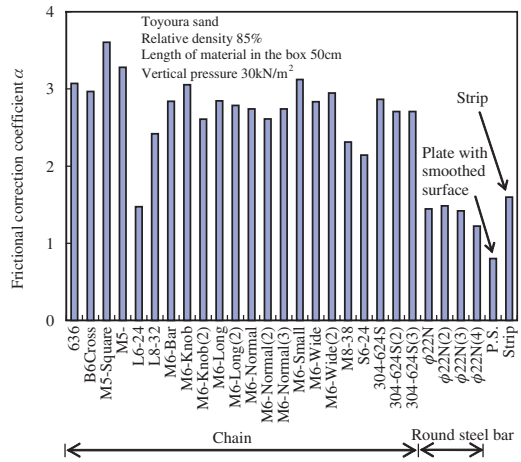

Figure 8. Variation of correcting factor with pullout force.

of steel plate with smooth surface was 1.5 kN and for the stripe with projection ranged from 8 kN to 9 kN. Although the resistances were plotted in large variety, the largest of the resistance of a particular material is taken compared with that of the strip with projection because of width effect. The resistance of plate with smooth surface is less than that of chain. This difference relating to both surface and type of plate describes the effect of shape on strength.

There can also be a different inspection for resistance, when focusing on the mechanism of resistance generation. Figure 8 indicates transformed values of the pullout force based on equations (3) and (4). The vertical earth pressure σ_v, measured in the fill is used for the calculation and not the load intensity applied on the cover plate of the box.

The vertical earth pressure measured close to the area surrounding the chain in the fill is found to be higher than the load intensity applied to the cover plate. This shows that the fill tends to swell due to dilatancy subject by pulling out the chain, however the swelling is restricted by the side wall effect.

As mentioned above, although the largest pullout resistance is obtained in the strip with projection, however, larger value of corrected friction factor is obtained in the chain. This means that the chain is more superior in generating resistance than the strip with projection. The variation of the friction correction factor for the various reinforcing materials used for the test is as shown in figure 8.

The frictional correction factor obtained for the various shapes of the chain ranged between 2.0 to 3.5 while that obtained for strip with projection was 1.6, for steel bar, the range was from 1.2 to 1.5, and for smooth steel plate it was 0.8.

Although the diameters of chains and round steel bars used for the test were the same (about 22 mm),

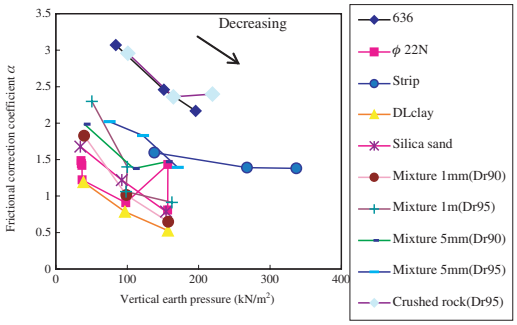

Figure 9. Decrease of resistance as confining pressure increases.

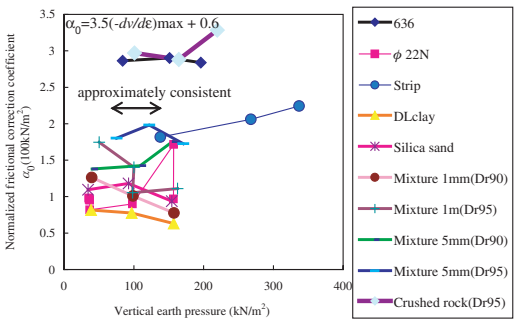

Figure 10. Normalized frictional correction factor by confining pressure.

the friction correction factors obtained for chains were larger than that of round steel bar. This is clear evidence that the reinforcement effect of the chain is more efficient.

Figure 9 shows the variation of the frictional correction factor with the measured vertical earth pressure. As the vertical earth pressure increases, the friction correcting factor tends to decrease although the surface and shape of different material are of concern. This decreasing behaviour of the frictional correcting factor can be corrected using equation (5) to give similar value almost independent of the confining pressure.

$$\alpha_0 = \alpha \times (\sigma_v / 100)^{0.4} \tag{5}$$

In this paper, the frictional correction factor adjusted at the stress of 100 kN/m^2 is called a normalized frictional correction factor α_0.

The adjustment is as shown in Figure 10 when normalization is done at the vertical earth pressure level of 100 kN/m^2 and raise a power factor 0.4 for the confining earth pressure as given in equation(5).

In this study, the normalized frictional correction factor is a parameter necessary for design of the steel

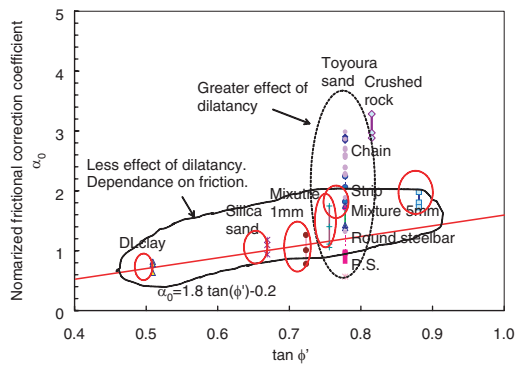

Figure 11. Design method considering dilatancy effect.

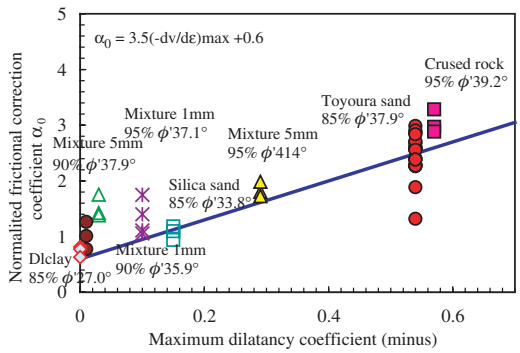

Figure 12. Dilatancy coefficient vs. correcting factor.

chain reinforcement. Its property is divided into two, one in which the effect of the dilatancy is expected and the other which is strongly affected by internal friction angle but dilatancy effect is not of concern.

Figure 11 shows relationship between the internal Friction angle and correction factor. A slope can be drawn through average data, if the vertical variation of data group is neglected at a friction coefficient of 0.8 that corresponding to Toyoura sand, crushed rocks and other soil types, while data for material type of smooth surface plate and round steel are plotted well along the estimation line.

Figure 12 shows the relationship between the dilatancy and the friction correction factor defined at the pressure 100 kN/m^2. The normalized friction correction factor with respect to chain tends to increase as an absolute value of the dilatancy coefficient increases. This relation for the increase in absolute value can be approximated by equation (7).

$$\alpha_0 = 1.8 \tan \phi' - 0.2 \tag{6}$$

$$\alpha_0 = 3.5\left(-\frac{dv}{d\varepsilon}\right) + 0.6 \tag{7}$$

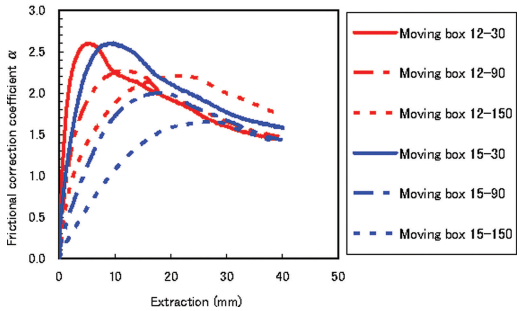

Figure 13. Curves figured by sliding box test results.

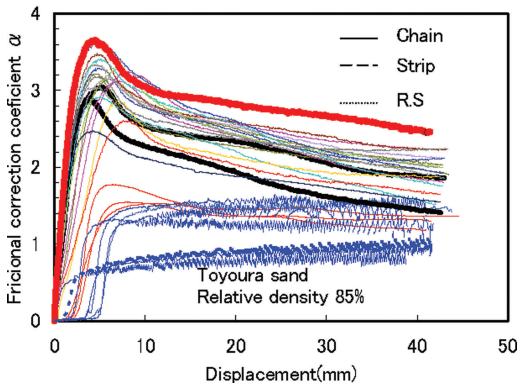

Figure 14. Curve modes subjected to standard pull out testing.

7 SLIDING BOX TEST RESULT

Figure 13 shows the relation between the frictional correction factor and the amount of extraction displacement of chain subject to the sliding box test. A set of shape of curve is divided into two groups; the first group consist of curves which have a hardening and sequent softening that well suits the behaviour of over consolidated soils, and the other group consists of curves with only hardening behaviour similar to the ones of normally consolidated soil. This phenomenon is similar to the standard test result shown in Figure 14.

Figure 13 are the result of test subjected to a vertical applied load of 30 kN/m^2 while figure 14 show a typical curve relating to standard test results. Comparing both figures, it is evident that the same curve patterns are obtained.

Figure 16 shows the relationship between normalized frictional correction factor and the ratio of confining earth pressure to the load intensity applied at the cover plate. The pressure ratio reveals a degree of dilatancy effect, because when the dilatancy effect is large, the ratio becomes larger. This figure shows the same trend for those obtained with the standard test results.

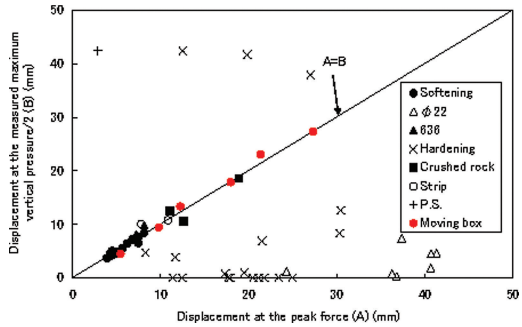

Figure 15. Maximum frictional correction coefficient and measured vertical earth pressure.

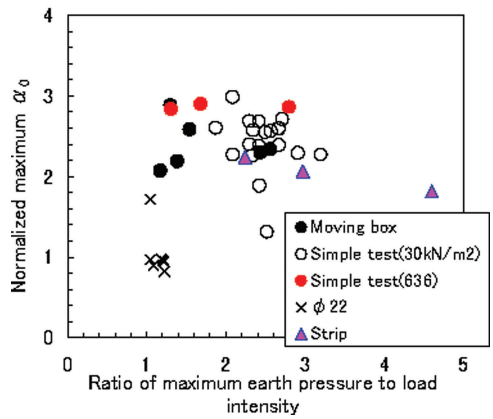

Figure 16. Frictional coefficient vs. earth pressure acting to chain.

Photo 2. Arrangement of chain and its attachments.

8 SITE CONSTRUCTION EXAMINATION

Photo 2 shows the chain arrangement work in the field for the installation of chain, anchor and the wall of steel frame set at the 50 cm spacing.

Photo 3. Completion of test embankment.

Photo 4. Affluent surrounded by green grass.

Photo 3 shows the figure of completed slope, and Photo 4 shows the growth of grass around the wall.

9 CONCLUSIONS

The sliding box test apparatus was made for trial purposes to examine the chain pullout resistance under standard condition and to compare the sliding box test properties with the standard test results. As a result, similar and compatible results were obtained from the both tests. From the result of both tests, the following points can be notes.

1) The governing operation for predicting resistance is summarized into the set of equations presented in this paper.
2) It is proved that the frictional correction factor can unify the degree of resistance among various kinds of reinforcements.
3) It was shown that the chain is a good reinforcement material that demonstrates the effect of dilatancy of the soil.
4) Similar characteristics in pullout test result generated in the standard test and sliding box test with regards to chain used are recognized.

REFERENCES

Fukuda M., Hongo T., Kitamura A., Mochizuki Y., Fujimura E., and Kimura M. (2006). "Dilatancy effect on pull out frictional force of chain", Proceedings of 7th National Symposium on Ground Improvement, The Society of Material Science, Japan, pp. 65–70 (In Japanese).

Fukuda M., Hongo T., Kitamura A., Mochizuki Y., and Kimura M. (2006). "General formuras of geosynthetic mechanics", Japan Chapter of International Geosynthetics Society, 21th Annual symposium (In Japanese).